Published in final edited form as:
Eur J Pharm Sci. 2010 January 31; 39(1-3): 103. doi:10.1016/j.ejps.2009.11.002.

Transport of Chitosan-DNA nanoparticles in human intestinal M-cell model versus normal intestinal enterocytes

Irina Kadiyala[1,3], **Yihua Loo**[1,2], **Krishnendu Roy**[1,4], **Janet Rice**[1], and **Kam W. Leong**[2]

[1] Department of Biomedical Engineering, Johns Hopkins University, Baltimore, MD 21205

[2] Department of Biomedical Engineering, Duke University, Durham, NC 27708

Abstract

Oral vaccination is one of the most promising applications of polymeric nanoparticles. Using two different *in vitro* cellular models to partially reproduce the characteristics of intestinal enterocytes and M-cells, this study demonstrates that nanoparticle transport through the M-cell co-culture model is 5 fold that of the intestinal epithelial monolayer, with at least 80% of the chitosan-DNA nanoparticles uptaken in the first 30 minutes. Among the properties of nanoparticles studied, ligand decoration has the most dramatic effect on the transcytosis rate: transferrin modification enhances transport through both models by 3–5 fold. The stability of the nanoparticles also affects transport kinetics. Factors which de-stabilize the nanoparticles, such as low charge (N/P) ratio and addition of serum, result in aggregation and in turn decreases transport efficiency. Of these stability factors, luminal pH is of great interest as an increase in pH from 5.5 to 6.4 and 7.4 leads to a 3 and 10 fold drop in nanoparticle transport respectively. Since soluble chitosan can act as an enhancer to increase paracellular transport by up to 60%, this decrease is partially attributed to the soluble chitosan precipitating near neutral pH. The implication that chitosan-DNA nanoparticles are more stable in the upper regions of the small intestine suggests that higher uptake rates may occur in the duodenum compared to the ileum and the colon.

Keywords

M-cells; chitosan nanoparticles; transcytosis; nonviral gene delivery; nanomedicine

1. Introduction

Polymeric nanoparticles are increasingly being used in the oral delivery of bioactive pharmaceuticals such as peptides, proteins and nucleic acids. Nanoparticles may enhance the oral bioavailability of encapsulated therapeutic moieties by facilitating internalization by cells. Cellular uptake in oral delivery is partially determined by particulate size, with particles smaller than 100nm favoring transcytosis, while particles above 1μm being trapped in the Peyer's patches (Desai et al. 1997; Jani et al. 1990), and particles greater than 10μm (Ermak et al. 1995) poorly absorbed. Polymeric nanoparticles are attractive drug carriers since their

Correspondence should be addressed to K.W. Leong, 136 Hudson Hall, Box 90281, Duke University, Durham, NC 27708, (919) 660-8466 (telephone), (919) 684-4488 (fax), kam.leong@duke.edu.
[3]Vertex Pharmaceuticals, Cambridge, MA 02139,
[4]Department of Biomedical Engineering University of Texas, Austin Austin, TX 78712

physiochemical characteristics (such as hydrophobicity, size, surface charge) can be modulated as a function of polymer design, thereby tailoring their drug release profile and biological behavior. Their specificity may also be augmented by surface ligand conjugation.

One of the most promising applications of polymeric nanoparticles is in the field of oral vaccination, which can induce both systemic and mucosal immune responses. Many groups have used cationic polymers to deliver antigenic peptides (Le Buanec et al. 2001; Roth-Walter et al. 2005; Salman et al. 2005), DNA (Chew et al. 2003; Roy et al. 1999) and adjuvants to lymphoid tissue (in particular, the lymphoid follicles and Peyer's patches) of the gut. In the Peyer's patches, M-cells which overlie the gut-associated lymphoid tissue are the primary targets of oral vaccine delivery. These specialized antigen-sampling epithelial cells are characterized by a high endocytic rate and low degradation ability. M-cells are capable of transporting a variety of materials, including nanoparticles (Garinot et al. 2007) and microparticles (Ermak et al. 1995; Jepson et al. 1993; van der Lubben et al. 2001), making them attractive portals for the oral delivery of therapeutics and for mucosal vaccination. While the mechanisms of particle uptake and transport are not well understood (des Rieux et al. 2005), several ligands have been shown to enhance particle uptake by intestinal M-cells (Brayden et al. 2005; Jepson et al. 1996; Roth-Walter et al. 2005). Particle uptake by M-cells is dependent on a variety of factors, such as particle size, surface charge, dosage, stability and ligand conjugation (O'Hagan 1996).

The objective of this study is to understand the interplay of factors which enhance the transcytosis of DNA nanoparticles across an *in vitro* model of M-cells, and to compare transport mediated by M-cells versus normal epithelial cells. The differentiated Caco-2 cells (Delie & Rubas 1997; Sambuy et al. 2005) and Caco-2-lymphocyte co-culture (Kerneis et al. 1997) are well-characterized cellular models of normal intestinal epithelium and M-cells respectively. Both systems have been extensively used to elucidate the unidirectional transport of diverse drugs and particles from the apical to the basolateral surface, and the data obtained correlate with *in vivo* experiments (Artursson 1990; Artursson & Karlsson 1991).

By applying the two *in vitro* models to the transport of chitosan-DNA nanoparticles, this study aims to clarify the influence of the intrinsic properties of the nanoparticles (such as polymer chain length, charge (nitrogen to phosphate, N/P) ratio, nanoparticle size and surface charge, ligand conjugation) and external conditions (pH, serum content) on transcytosis rate. Although the effects of particle size on particle transport are well-studied, the majority of studies are performed using latex and polystyrene beads, which have vastly differing surface properties from biodegradable polymers typically used to deliver therapeutic agents. Current literature reflects the pervasive use of PLGA and chitosan particles in oral vaccination strategies. In particular, chitosan nanoparticles are attractive gene and protein carriers as the polymer is mucoadhesive and enhances paracellular permeability (Bowman K 2006; Lin et al. 2007) by opening the tight junctions between epithelial cells. Although chitosan nanoparticles and microparticles have been extensively studied in either Caco-2 cells or Caco-2-lymphocyte cells, no comparison (qualitative or quantitative) between the two models has been made. This paper also demonstrates that the type of polymer used to synthesize the nanoparticles, as well as the ligand conjugation, plays a role in altering transcytosis through the intestinal epithelium.

2. Materials and Methods

2.1. Materials

2.1.1. Cell lines—Human colon carcinoma Caco-2 cell line was obtained from the American Type Culture Collection (ATCC) (Rockville, MD). Cells from passage 72–92 were used for the transport studies.

2.1.2. Cell culture reagents and chemicals—Eagle's minimum essential media with 2mM L-glutamine and Earle's BSS, supplemented with 20% fetal bovine serum and 1% penicilin-streptomycin, were purchased from Gibco™ Invitrogen (Carlsbad, CA). Low molecular weight chitosan (60 to 100 kDa) was purchased from Pronova Biopolymers (Norway), while high molecular weight chitosan (390 kDa) was a gift from Vanson Chemicals (Redmond, WA). The plasmid used to form the nanoparticles, p43LacZ, was obtained from Dr. Barry Bryne, University of Florida, FL. Carboxylate-modified 0.2 micron fluorescent beads were purchased from Molecular Probes (Eugene, OR). Alpha-malemidyl-w-N-hydroxysuccinimide (MH) polyethylene glycol and succinidyl succinamade of methoxy polyethylene glycol (SSH) were from Nektar Therapeutics (Huntsville, AL).

2.2. Methods

2.2.1. Isolation of lymphocytes from Peyer's patches—Peyer's patches were first dissected from female Balb/c mice. The isolated lymphoid tissue was then ground on a cell strainer (70μm, nylon mesh, Becton Dickinson, Franklin Lakes, NJ). The resulting cell suspension was centrifuged at 500rpm for 50 seconds to remove cell aggregates, and followed by another centrifugation at 500rpm for 10 minutes to pellet the cells. The lymphocytes were finally re-suspended at a concentration of 10^7 cells per milliliter of culture media.

2.2.2. Cell culture—Caco-2 cells were expanded as recommended by ATCC. Upon reaching 80% confluence, Caco-2 cells were harvested by trypsinization, washed and resuspended in culture medium. 3×10^5 cells were then seeded onto the lower face of a Transwell (6.5mm diameter, 3.0 micron pore-size membrane) (Costar, Cambridge, MA). The co-culture protocol was adapted from Pringaul et al. (Kerneis et al. 1997). After 2 weeks of growth, freshly isolated lymphocytes from Peyer's patches (PLL) of Balb/c mice (6 to 7 weeks of age obtained from Charles River Laboratories, Wilmington, MA) were added at a concentration of 10^6 cells per well to the upper chamber of the Transwell. The co-culture was maintained for the next 3 days, though the upper chamber of the inserts was rinsed with 0.1M Dulbecco PBS (DPBS) daily.

2.2.3. Preparation and characterization of DNA nanoparticles—Chitosan DNA nanoparticles were prepared using high (HMW) and low (LMW) molecular weights of chitosan at various concentrations, as previously described (Leong et al. 1998). Briefly, 10μg of DNA was added to 100μL of 50mM sodium sulphate and subsequently mixed with 100μL of chitosan solution under high-speed vortexing. The reaction was conducted at 55°C. The zeta-size and potential of the nanoparticles were measured using a Zetasizer-3000 (Malvern Instruments, Southborough, MA). Chitosan nanoparticles were also surface-modified by conjugating transferrin as previously described (Mao et al. 2001). Size separation of the nanoparticle suspension was performed via a two-step centrifugation in 70% and 85% sucrose in a 4:1 ratio, at 14,000g for 6 minutes and then 8,000g for 5 minutes. Under these conditions, fractions of nanoparticles in the range of 50–100nm, 200–250nm, and 400–500nm were obtained.

The gelatin DNA nanoparticles were synthesized according to previously published protocol (Truong-Le et al. 1999). PEI polyplexes were synthesized with 25 KDa branched PEI at a N/P ratio of 10. Carboxylate-modified 0.2 micron fluorescent polystyrene beads were purchased from Molecular Probes (Eugene, OR).

2.2.4. Transport Studies—The transepithelial electrical resistance (TEER) of each cellular insert was determined by means of a Millicell-ERS (Millipore Corporation, Bedford, MA). This is to ensure the intactness of the cell layers. All transport studies were conducted at 37° C. Samples (nanoparticles containing 15 μg DNA in 300 μl) were placed in the bottom chamber of a well and an equal volume of transport medium added to the top chamber. At set time points, 200 μl of the medium was collected from the apical chamber and replaced with fresh medium.

As the DNA-chitosan nanoparticles were labeled with TOPRO-1 (Molecular Probes Invitrogen, Carlsbad, CA), flow cytometry (Beckton-Dickinson, Franklin Lakes, NJ) was used to detect their presence in the media collected. The FL1 signal was measured for 30 seconds, and after background subtraction (using media collected from cells to which no nanoparticles were added), the accumulated events were expressed as events per minute per area of insert. The cumulative percent of events was then calculated based on the original concentration of nanoparticles. Aliquots of the media in the upper chamber were desalted and concentrated via dialysis in a Slide-A-Lyser cassette (Pierce, Rockford, CA), in order to determine the intactness of the DNA present in the nanoparticles that were transported across the cell layer. Following dialysis, the samples were treated with chitosanase in acetate buffer at pH 5.5 in order to release the DNA from the nanoparticle. The treated samples were then applied onto 0.8% agarose gel to appraise the condition of the plasmid DNA. All the transport studies were performed in triplicate and for the flow cytometry measurements, all three samples were pooled.

2.2.5. Immunohistochemistry—At the end of the transport studies, the cells were fixed in 4% formaldehyde. The cellular inserts were washed in PBS thrice, and 10% normal goat serum was added to suppress non-specific binding of anti-bodies for 15 minutes. Rabbit anti-Ulex Europaeus lectin type 1 (DAKO Corporation, CA) was then added for 1 hour to detect the M cells, followed by three PBS washes before the secondary rhodamine conjugated Goat anti - Rabbit IgG (Fisher Scientific, PA) was added for 30 minutes. The nuclei were also stained using DaPi (Molecular Probes Invitrogen, Carlsbad, CA). The supporting layer under the cells was separated from the insert and mounted on cover glass for visualization under confocal microscopy (Carl Zeiss, Thornwood, NY).

3. Results

3.1. Integrity of Caco-2-PLL cellular co-cultures

Caco-2 cells were cultured for 14 days on the insert in order for them to fully differentiate. Although some studies (Vachon & Beaulieu 1992) reported that Caco-2 cells grown on inserts are fully differentiated by 25 days, a shorter duration was used as pilot studies revealed no difference in transport rates between cells cultured for 14 or 25 days. Prior to adding the lymphocytes, the intactness of the Caco-2 cellular layer was checked by determining their transepithelial electrical resistance (TEER). The average TEER value after 14 days was 250 ± 20 Ohm cm^2. Subsequent addition of lymphocytes did not significantly alter the TEER. As a precaution, the isolated and processed lymphocytes were analysed by flow cytometry and the ratio of B to T lymphocytes was found to be 63:37. This is consistent with published results for PLL follicle cells (MacDonald & Carter 1982) and suggests that the isolated cells were mostly the desired B cells.

To ensure that the buffer solution would not compromise the integrity of the cellular inserts, control cells were immersed in the buffer for 2 hours under the same conditions and the TEER measured. The average TEER value for untreated Caco-2 layer after growing for 2 weeks in 0.1M DPBS (pH 5.5) was 450 ± 36 Ohm*cm^2. This confirmed that the integrity of cell layer would not change under the experimental conditions. In addition, analysis of aggregation kinetics of the chitosan DNA nanoparticles by Zetasizer did not detect any significant increase in average size or size distribution of the nanoparticle within two hours of immersion in 0.1M DPBS buffer (pH 5.5), indicating there would be distinct non-aggregated nanoparticles available for transcytosis.

3.2. Characterization of Chitosan-DNA Nanoparticles

The size and zeta potential of the chitosan nanoparticles with different N/P ratios are shown in Figure 1. The LMW chitosan-DNA nanoparticles were slightly larger than HMW chitosan-

DNA nanoparticles at N/P ratios above 6, but the difference was not statistically significant. In contrast, the zeta potential increased more dramatically with increasing N/P ratio for LMW as compared to HMW chitosan.

3.3. Transport of Chitosan-DNA Nanoparticles

Confocal microscopy confirmed the transport of chitosan-DNA nanoparticles through the cell layer. Figure 2A is an orthogonal confocal scan through cells grown on the Transwell membrane and incubated for 30 minutes with chitosan nanoparticles (labeled red). The chitosan nanoparticles were localized within the cell layers, indicating that uptake and transcytosis occurred through the cell layer. However, the DNA complexed to chitosan underwent significant degradation after transcytosis through the Caco-2-PPL co-culture. Gel electrophoresis of the DNA extracted from the nanoparticles revealed many low molecular weight bands (Figure 2B).

Figure 3 is a comprehensive overview of the transport of nanoparticles through the Caco-2 layer alone in comparison to the Caco-2-PLL co-culture. In general, more nanoparticles were transported through the cellular layer in the presence of lymphocytes, and for longer durations. For HMW chitosan, in the presence of lymphocytes, nanoparticles with low N/P ratios showed a high rate of transport. In contrast, in Caco-2 cells without lymphocytes, nanoparticles showed higher transport at N/P ratios of 9 and 12 but became negligible at N/P ratios of 1.5 and 3. For LMW chitosan, the transport at all concentrations was comparable in the co-culture system; while in the absence of PLL, transport of nanoparticles increased with N/P ratio. In both the Caco-2 and Caco-2-PLL systems, the transport of HMW chitosan nanoparticles was 2–4 fold higher than that exhibited by LMW chitosan. In both cellular systems, the transport exhibited a behavior typical of that governed by the Michaelis-Menton, saturable kinetics, where at least 80% of the total nanoparticles was transcytosed in the first 30 min.

Figure 4 shows the TEER values upon addition of the HMW chitosan nanoparticles. The TEER dropped drastically by 300–400 ohm cm^2 within 30 minutes and then continued to decline slowly over the next 2 hours. The presence or absence of PLL did not affect the TEER changes, but higher N/P ratio induced a steeper drop. The change in TEER was comparable for both HMW and LMW (supplementary data) chitosan nanoparticles. Interestingly, the addition of free LMW chitosan (up to 0.05 and 0.025 %) did not noticeably affect the transport through the layer with M cells, although the transport through the layer of Caco-2 cells alone did (data not shown). Earlier studies have shown that soluble chitosan augments paracellular transport by opening tight junctions between epithelial cells (Artursson et al. 1994;Lin et al. 2007).

3.4. Effect of pH and Serum on the Efficiency of Nanoparticle Transport

To study the effect of pH, transport studies were conducted in 0.1M DPBS over the pH range of 5.5 – 7.4 in Figure 5A. The cell layer integrity is known to be maintained in this pH range (Palm et al. 1999). For both HMW (Figure 5A) and LMW (data not shown) chitosan nanoparticles, the highest rate of transport occurred at pH 5.5, in both the Caco-2 and the Caco-2-PLL cell layers. Increasing the pH decreased the transport efficiency by 3-fold and 10-fold at pH 6.4 and 7.4, respectively. A plausible reason for the drop in transport efficiency is nanoparticle aggregation which occurs at the higher pHs. Likewise, transport efficiency decreased at 2 or 10% serum concentrations, possibly due to nanoparticle aggregation induced by serum proteins.

3.5. Transport of Nanoparticles as a Function of Size

As suggested by experiments in high serum media, the smaller nanoparticles were transported more efficiently across the cell layers. As depicted in figure 5B, the sub-population of 50–100 nm nanoparticles had a transport rate 1.5 times over the non-fractionated control. There was

no significant difference in transport for other fractions of nanoparticles as compared to the control.

3.6. Effect of Transferrin Modification of Nanoparticles on the Efficiency of Transport

Many studies harness receptor-ligand interactions to improve cellular uptake and transport. To study the validity of this assumption in oral delivery, transferrin was conjugated to chitosan DNA nanoparticles formed at N/P ratio of 3. Transferrin receptors are present on Caco-2 cells, and transferrin conjugation enhances transcytosis of viral vectors (Zhu et al. 2004). After conjugation and dialysis, the transferrin-decorated nanoparticles had an average size of 499 nm, in two sub-populations of 200 and 900 nm. The latter mostly comprised of aggregates. The control group (without transferrin) was also subjected to the same crosslinking reaction, fractionation in sucrose gradient and dialysis. The transferrin conjugation increased the zeta potential at pH 5.8 from 20 ± 1.2 mV to 35 ± 0.8 mV. At pH 7.4, the zeta potentials were comparable at 14.5 ± 0.8 mV and 15.8 ± 1.4 mV for unmodified and transferrin-conjugated nanoparticles, respectively.

Transferrin decoration enhanced the transport of nanoparticles through both types of cell layers by 3- to 5-fold, as depicted in Figure 6. Similar to early studies on unmodified nanoparticles, the enhancement effect of the presence of lymphocytes was clear for all samples (data not shown). Interestingly the optimal pH for transport was 6.5 for these transferrin-decorated nanoparticles, as opposed to pH 5.5 in previous studies with undecorated nanoparticles. The transferrin modification might affect the surface characteristics as well as the stability of the nanoparticles, although the exact reason for this different behavior is not known at this point. The surface density of transferrin also could not be accurately characterized. It is likely that the carbodiimide coupling reaction used to conjugate transferrin could also crosslink the chitosan and led to higher stability of the nanoparticles at higher pH.

Unfortunately, ligand decoration did not improve nanoparticle transport significantly in the presence of serum. Like the unmodified nanoparticles, the transport efficiency decreased when serum concentration was raised. At low (2%) serum medium, a low transport rate of 0.5% was detected only in the presence of PLL. At 10% serum level, the transport was negligible. This decrease was attributed to aggregation of the nanoparticles in the presence of serum proteins.

3.7. Transport of Nanoparticles Synthesized from Various Polymers

To explore the effect of the nature of the nanoparticles on transport, we studied different nanoparticles, whose properties are tabulated in Table 1. There was unavoidable variation in the number of nanoparticles used in the experiments because of differences in particle size and N/P ratio. We kept the DNA dose constant and have established that at particulate concentrations containing 15 μg of DNA, the transport rate would be at the maximum with respect to the particular type of nanoparticles. In Caco-2 cell layers without lymphocytes, minimal transport was observed regardless of nanoparticle composition. In Caco-2-PLL co-cultures, transferrin-conjugated nanoparticles showed significantly greater transport rate compared to unmodified controls. Amongst the unmodified nanoparticles, the transport of chitosan nanoparticles was slightly better than that of polystyrene and PEI nanoparticles.

4. Discussion

The polarized Caco-2 cell model has been widely used in *in vitro* studies of epithelial transport processes, due to its homology to human intestinal epithelial absorptive enterocytes (Artursson 1990; Hilgers et al. 1990). However, it is a homogenous cell system consisting solely of absorptive cells, and its behaviour is not representative of the different sections of the intestinal tract. In contrast, the infiltration of lymphocytes into the polarized Caco-2 cells in a co-culture

model triggers the Caco-2 to further differentiate into an M-cell phenotype. M-cells are specialized for transport of antigens and intact nano- and microparticles to the underlying immune cells, and are thus a more appropriate model for studying transcytosis of particulate therapeutics in the context of oral vaccination. In our studies, the M-cell model demonstrates higher transcytosis rates of approximately five times more particles across the cell layer compared to normal enterocytes, for all the different kinds of nanoparticles studied. This is consistent with results published by Lai and D'Souza(Lai & D'Souza 2008) in which M-cell like cultures transported three times more microparticles than Caco-2 cultures. The extremely low transcytosis rate across Caco-2 cell layer in the absence of lymphocytes was also observed by Van der Lubben et al.(van der Lubben et al. 2002). These results suggest that in the local region of the Peyer's patches, M-cells are primarily responsible for uptake.

A range of factors affect the transport of nanoparticles from the luminal side to the basolateral side. Of these, the pH of the luminal environment is of great significance as the pH of the intestinal tract changes from approximately 6 in the duodenum to 7.5 in the ileum. This implies that the transport of nanoparticles through M-cells of the lymphoid follicles in the duodenum will differ from that of the Peyer's patches in the ileum. It also has great implications for oral delivery of unprotected nanoparticles administered orally. This study is the first to investigate the effects of pH on intestinal epithelial transport; increasing pH decreases transcytosis, for a variety of reasons. Higher pH, above 6, promotes aggregation of these types of DNA nanoparticles. From studying the size dependency of transcytosis, increasing the size from 100nm to 500nm results in a drop in transport efficiency. Another plausible reason is that increasing the pH of the environment de-stabilizes the nanoparticles. This explains why crosslinking nanoparticles (in the studies involving transferrin conjugation) leads to a higher transcytosis rate compared to unmodified nanoparticles. The same reason applies to comparisons of HMW and LMW chitosan nanoparticles. LMW nanoparticles are less stable at the lower N/P ratios and so do not transport as well as HMW nanoparticles. A less stable nanoparticle delivers the DNA payload to the enterocyte, as opposed to the intact nanoparticle being transcytosed to the underlying cells.

Chitosan enhances the permeability of the intestinal epithelium by opening the tight junctions between cells (Lin et al. 2007). Since chitosan is added in excess in forming the nanoparticles, free chitosan may have an enhancer effect on nanoparticle transcytosis, evident from the decrease in TEER following addition of chitosan nanoparticles. At high pH, the free chitosan precipitates, resulting in a drop in the permeability effect and hence transcytosis rate. Consequently, the optimal pH is 5.5, which corresponds to the pH that can readily solubilize HMW chitosan.

The enhancer effect also explains the higher transcytosis rate of chitosan nanoparticles with higher N/P ratios, as well as of chitosan nanoparticles compared to gelatin, carboxylated polystyrene and polyethyleneimine (PEI). Since chitosan, gelatin and PEI are positively charged and carboxylated polystyrene is negatively charged, the surface charge of the nanoparticle might not be as significant as the stability of the nanoparticle. The transcytosis of PEI nanoparticles is probably compromised by its instability in the endosomal compartment of the cell. Thus, PEI may be a good gene carrier, but not for delivering intact nanoparticles to the underlying lymphoid cells for immunization.

5. Conclusion

Using two different *in vitro* cellular models to partially reproduce the characteristics of intestinal enterocytes and M-cells, this study demonstrates the importance of M-cells on nanoparticle transcytosis for oral gene delivery. As expected, ligand conjugation improves transcytosis for both normal enterocytes and M-cells to the same extent. More significantly,

ligand conjugation has the most dramatic effect on transcytosis rate compared to other intrinsic properties of nanoparticles. pH also plays an important role in the transcytosis of chitosan DNA nanoparticles. The observation of maximal nanoparticle transcytosis occurring at 5.5 suggests that uptake in the lymphoid follicles of the duodenum could play a more significant role compared to Peyer's patches. This study suggests that future macro-formulation design to deliver nanoparticles to the GI tract may want to take this *in vitro* finding into consideration. It also sets the foundation for further nanoparticle optimization to help realize the potential of nonviral oral gene delivery.

Supplementary Material

Refer to Web version on PubMed Central for supplementary material.

Acknowledgments

Support by NIH (HL89764) is acknowledged.

References

Artursson P. Epithelial transport of drugs in cell culture. I: A model for studying the passive diffusion of drugs over intestinal absorptive (Caco-2) cells. J Pharm Sci 1990;79:476–82. [PubMed: 1975619]

Artursson P, Karlsson J. Correlation between oral drug absorption in humans and apparent drug permeability coefficients in human intestinal epithelial (Caco-2) cells. Biochem Biophys Res Commun 1991;175:880–5. [PubMed: 1673839]

Artursson P, Lindmark T, Davis SS, Illum L. Effect of chitosan on the permeability of monolayers of intestinal epithelial cells (Caco-2). Pharm Res 1994;11:1358–61. [PubMed: 7816770]

Bowman KLK. Chitosan nanoparticles for oral drug and gene delivery. International J Nanomedicine 2006;1:117–128.

Brayden DJ, Jepson MA, Baird AW. Keynote review: intestinal Peyer's patch M cells and oral vaccine targeting. Drug Discov Today 2005;10:1145–57. [PubMed: 16182207]

Chew JL, Wolfowicz CB, Mao HQ, Leong KW, Chua KY. Chitosan nanoparticles containing plasmid DNA encoding house dust mite allergen, Der p 1 for oral vaccination in mice. Vaccine 2003;21:2720–9. [PubMed: 12798609]

Delie F, Rubas W. A human colonic cell line sharing similarities with enterocytes as a model to examine oral absorption: advantages and limitations of the Caco-2 model. Crit Rev Ther Drug Carrier Syst 1997;14:221–86. [PubMed: 9282267]

des Rieux A, Ragnarsson EG, Gullberg E, Preat V, Schneider YJ, Artursson P. Transport of nanoparticles across an in vitro model of the human intestinal follicle associated epithelium. Eur J Pharm Sci 2005;25:455–65. [PubMed: 15946828]

Desai MP, Labhasetwar V, Walter E, Levy RJ, Amidon GL. The mechanism of uptake of biodegradable microparticles in Caco-2 cells is size dependent. Pharm Res 1997;14:1568–73. [PubMed: 9434276]

Ermak TH, Dougherty EP, Bhagat HR, Kabok Z, Pappo J. Uptake and transport of copolymer biodegradable microspheres by rabbit Peyer's patch M cells. Cell Tissue Res 1995;279:433–6. [PubMed: 7895280]

Garinot M, Fievez V, Pourcelle V, Stoffelbach F, des Rieux A, Plapied L, Theate I, Freichels H, Jerome C, Marchand-Brynaert J, Schneider YJ, Preat V. PEGylated PLGA-based nanoparticles targeting M cells for oral vaccination. J Control Release 2007;120:195–204. [PubMed: 17586081]

Hilgers AR, Conradi RA, Burton PS. Caco-2 cell monolayers as a model for drug transport across the intestinal mucosa. Pharm Res 1990;7:902–10. [PubMed: 2235888]

Jani P, Halbert GW, Langridge J, Florence AT. Nanoparticle uptake by the rat gastrointestinal mucosa: quantitation and particle size dependency. J Pharm Pharmacol 1990;42:821–6. [PubMed: 1983142]

Jepson MA, Clark MA, Foster N, Mason CM, Bennett MK, Simmons NL, Hirst BH. Targeting to intestinal M cells. J Anat 1996;189(Pt 3):507–16. [PubMed: 8982824]

Jepson MA, Simmons NL, O'Hagan DT, Hirst BH. Comparison of poly(DL-lactide-co-glycolide) and polystyrene microsphere targeting to intestinal M cells. J Drug Target 1993;1:245–9. [PubMed: 8069566]

Kerneis S, Bogdanova A, Kraehenbuhl JP, Pringault E. Conversion by Peyer's patch lymphocytes of human enterocytes into M cells that transport bacteria. Science 1997;277:949–52. [PubMed: 9252325]

Lai YH, D'Souza MJ. Microparticle transport in the human intestinal M cell model. J Drug Target 2008;16:36–42. [PubMed: 18172818]

Le Buanec H, Vetu C, Lachgar A, Benoit MA, Gillard J, Paturance S, Aucouturier J, Gane V, Zagury D, Bizzini B. Induction in mice of anti-Tat mucosal immunity by the intranasal and oral routes. Biomed Pharmacother 2001;55:316–20. [PubMed: 11478583]

Leong KW, Mao HQ, Truong-Le VL, Roy K, Walsh SM, August JT. DNA-polycation nanospheres as non-viral gene delivery vehicles. J Control Release 1998;53:183–93. [PubMed: 9741926]

Lin YH, Mi FL, Chen CT, Chang WC, Peng SF, Liang HF, Sung HW. Preparation and characterization of nanoparticles shelled with chitosan for oral insulin delivery. Biomacromolecules 2007;8:146–52. [PubMed: 17206800]

MacDonald TT, Carter PB. Isolation and functional characteristics of adherent phagocytic cells from mouse Peyer's patches. Immunology 1982;45:769–74. [PubMed: 7068173]

Mao HQ, Roy K, Troung-Le VL, Janes KA, Lin KY, Wang Y, August JT, Leong KW. Chitosan-DNA nanoparticles as gene carriers: synthesis, characterization and transfection efficiency. J Control Release 2001;70:399–421. [PubMed: 11182210]

O'Hagan DT. The intestinal uptake of particles and the implications for drug and antigen delivery. J Anat 1996;189(Pt 3):477–82. [PubMed: 8982819]

Palm K, Luthman K, Ros J, Grasjo J, Artursson P. Effect of molecular charge on intestinal epithelial drug transport: pH-dependent transport of cationic drugs. J Pharmacol Exp Ther 1999;291:435–43. [PubMed: 10525056]

Roth-Walter F, Bohle B, Scholl I, Untersmayr E, Scheiner O, Boltz-Nitulescu G, Gabor F, Brayden DJ, Jensen-Jarolim E. Targeting antigens to murine and human M-cells with Aleuria aurantia lectin-functionalized microparticles. Immunol Lett 2005;100:182–8. [PubMed: 15913790]

Roy K, Mao HQ, Huang SK, Leong KW. Oral gene delivery with chitosan--DNA nanoparticles generates immunologic protection in a murine model of peanut allergy. Nat Med 1999;5:387–91. [PubMed: 10202926]

Salman HH, Gamazo C, Campanero MA, Irache JM. Salmonella-like bioadhesive nanoparticles. J Control Release 2005;106:1–13. [PubMed: 15970347]

Sambuy Y, De Angelis I, Ranaldi G, Scarino ML, Stammati A, Zucco F. The Caco-2 cell line as a model of the intestinal barrier: influence of cell and culture-related factors on Caco-2 cell functional characteristics. Cell Biol Toxicol 2005;21:1–26. [PubMed: 15868485]

Truong-Le VL, Walsh SM, Schweibert E, Mao HQ, Guggino WB, August JT, Leong KW. Gene transfer by DNA-gelatin nanospheres. Arch Biochem Biophys 1999;361:47–56. [PubMed: 9882427]

Vachon PH, Beaulieu JF. Transient mosaic patterns of morphological and functional differentiation in the Caco-2 cell line. Gastroenterology 1992;103:414–23. [PubMed: 1634060]

van der Lubben IM, van Opdorp FA, Hengeveld MR, Onderwater JJ, Koerten HK, Verhoef JC, Borchard G, Junginger HE. Transport of chitosan microparticles for mucosal vaccine delivery in a human intestinal M-cell model. J Drug Target 2002;10:449–56. [PubMed: 12575734]

van der Lubben IM, Verhoef JC, van Aelst AC, Borchard G, Junginger HE. Chitosan microparticles for oral vaccination: preparation, characterization and preliminary in vivo uptake studies in murine Peyer's patches. Biomaterials 2001;22:687–94. [PubMed: 11246962]

Zhu ZB, Makhija SK, Lu B, Wang M, Rivera AA, Preuss M, Zhou F, Siegal GP, Alvarez RD, Curiel DT. Transport across a polarized monolayer of Caco-2 cells by transferrin receptor-mediated adenovirus transcytosis. Virology 2004;325:116–28. [PubMed: 15231391]

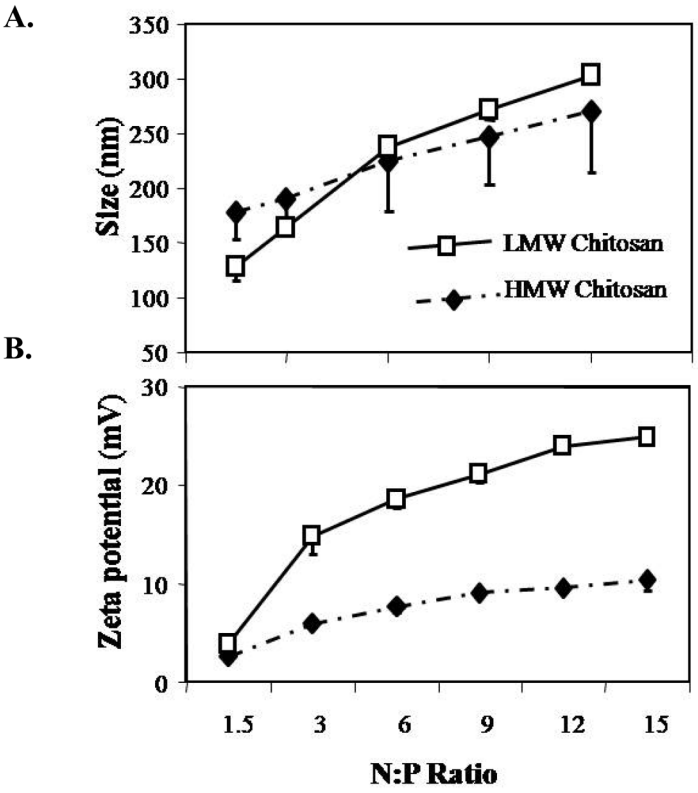

Figure 1. Physical characteristics of Chitosan-DNA Nanoparticles

(A) Size and (B) Zeta potential of nanoparticles as a function of the charge (nitrogen to phosphate, N/P) ratio. (Closed Diamond = HMW chitosan nanoparticles, Open square = LMW chitosan nanoparticles)

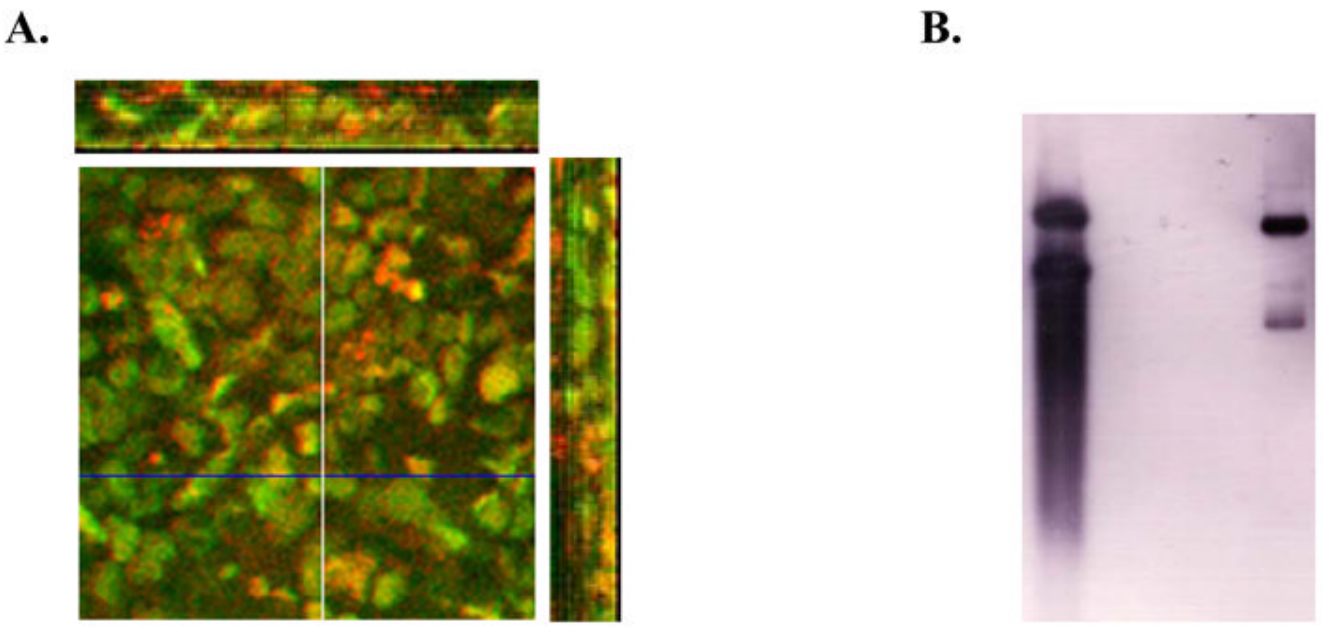

Figure 2. Uptake and transcytosis of chitosan-DNA nanoparticles

(A) Confocal image of Caco-2-lymphocyte co-cultures incubated with fluorescent labeled chitosan nanoparticles for 30 minutes. Cell nuclei were stained with DAPI (green) while the nanoparticles were labeled with To-Pro (red). Uptake occurred within 30 minutes as evident by intracellular localization of the nanoparticles. **(B) Gel electrophoresis of DNA extracted from transcytosed chitosan nanoparticles (left lane) compared to the control plasmid (right lane).**

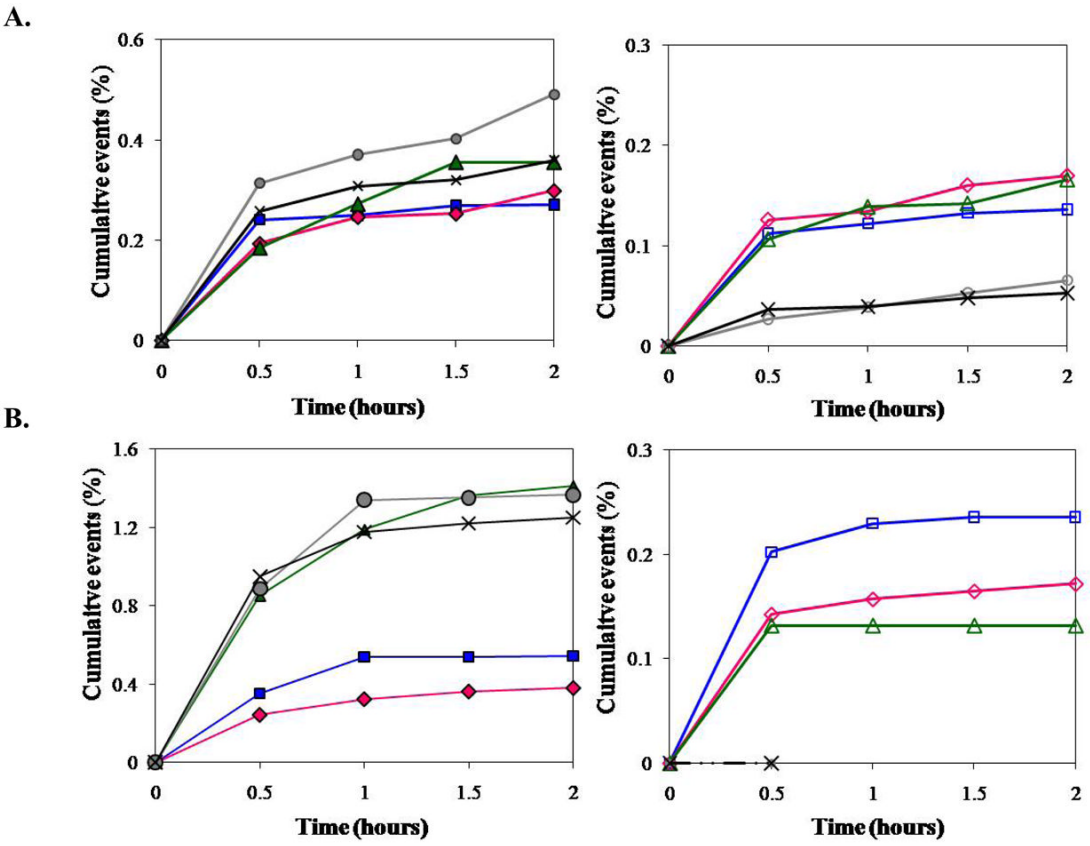

Figure 3.

Transport of (A) HMW (390kDa) and (B) LMW (60–100kDa) chitosan nanoparticles at different N/P ratios, in the presence and absence of Peyer's patch lymphocytes (Square = 12, Diamond = 9, Triangle = 6, Circle = 3, Cross = 1.5; Open symbols represent Caco-2 samples while closed symbols represent Caco-2-lymphocyte samples)

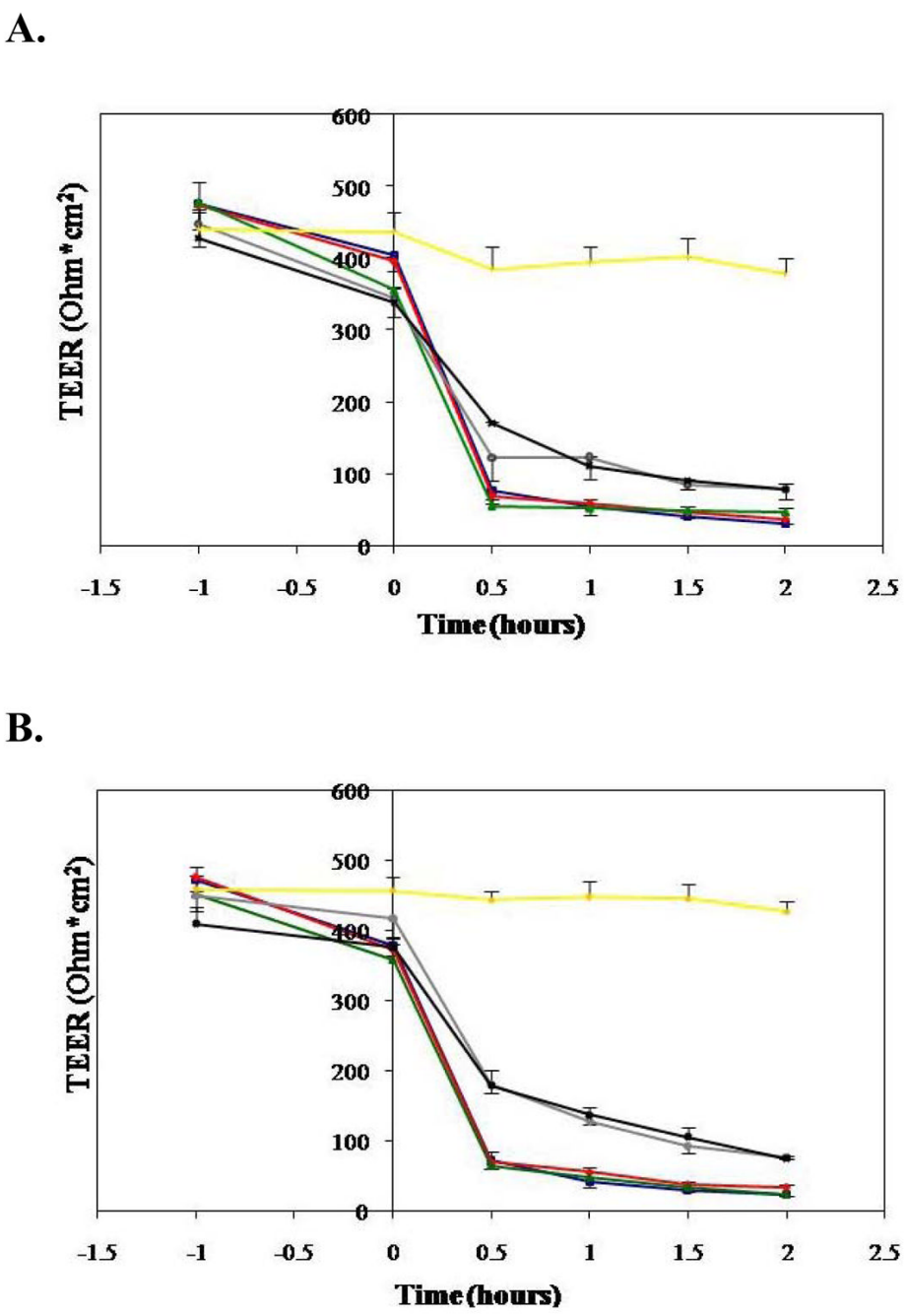

Figure 4.

Transepithelial electrical resistance of (A) Caco-2 and (B) Caco-2-lymphocyte co-culture changes upon addition of HMW chitosan nanoparticles of different N/P ratios (Square = 12, Diamond = 9, Triangle = 6, Circle = 3, Cross = 1.5, + = control; Open symbols represent Caco-2 samples while closed symbols represent Caco-2-lymphocyte samples)

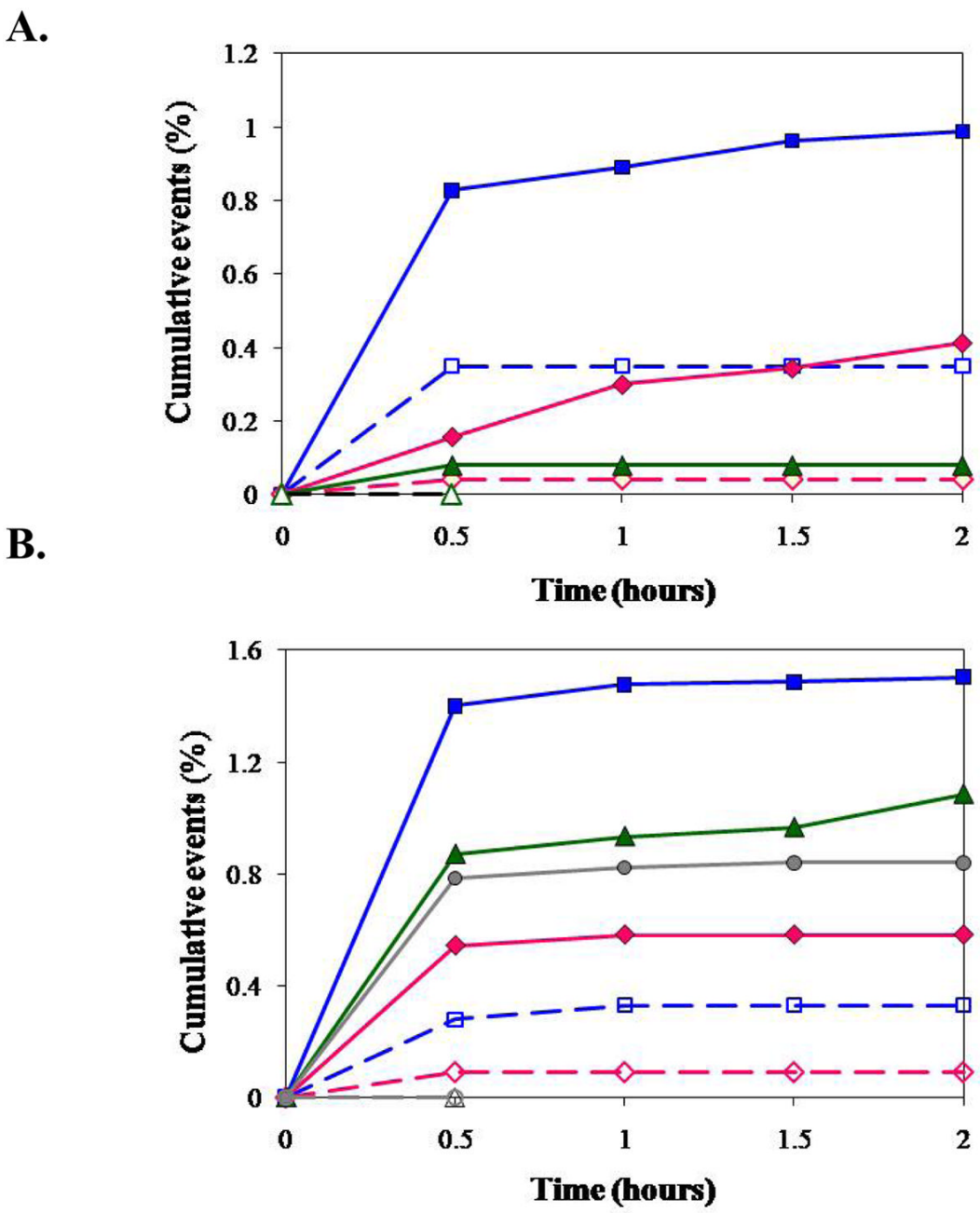

Figure 5.

Transport of HWM chitosan nanoparticles (N/P = 3) as a function of (A) pH of buffer medium (Square = pH 5.5, Diamond = pH 6.5, Triangle = pH 7.4; Open symbols represent Caco-2 samples while closed symbols represent Caco-2-lymphocyte samples)**, and (B) size** (Square = 50–100nm, Diamond = 200nm, Triangle = 400–500nm, circle = control; Open symbols represent Caco-2 samples while closed symbols represent Caco-2-lymphocyte samples).

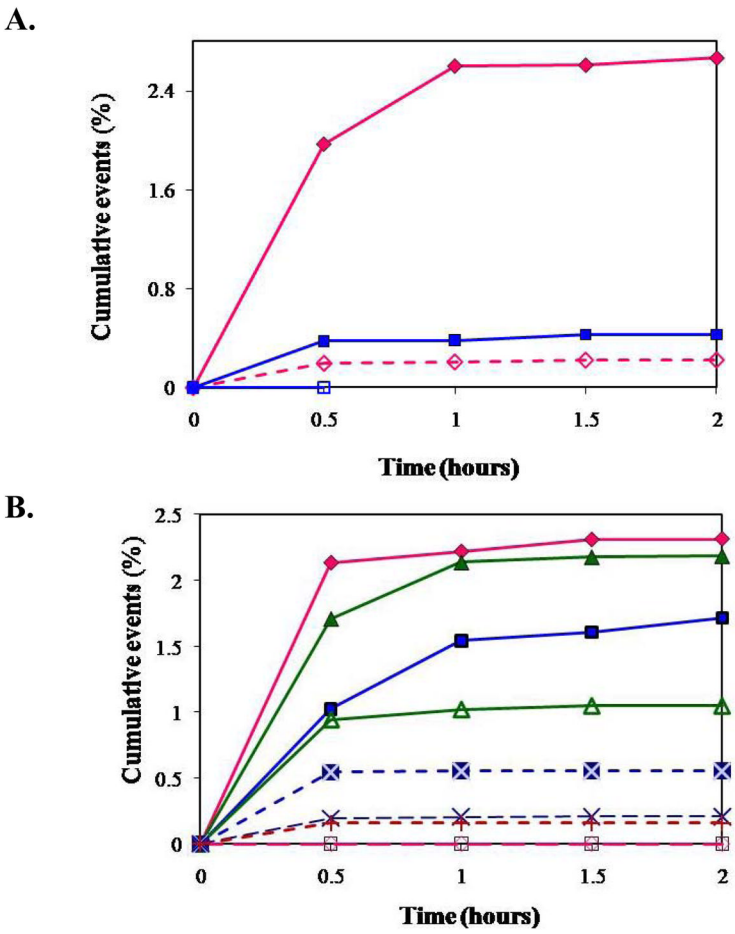

Figure 6. Transport of HWM chitosan nanoparticles (N/P = 3) with transferrin conjugation
(A) Transport of transferrin conjugated nanoparticles vs unmodified nanoparticles (Square = nanoparticles without modifications, Diamond = nanoparticles with transferrin conjugation; Open symbols represent Caco-2 samples while closed symbols represent Caco-2-lymphocyte samples) **(B) Transferrin conjugation modulates the transcytosis of nanoparticles under different pH and serum conditions.** (Square = pH 5.5, Diamond = pH 6.5, Triangle = pH 7.4, x = low serum media, + = high serum media; Open symbols represent Caco-2 samples while closed symbols represent Caco-2-lymphocyte samples)

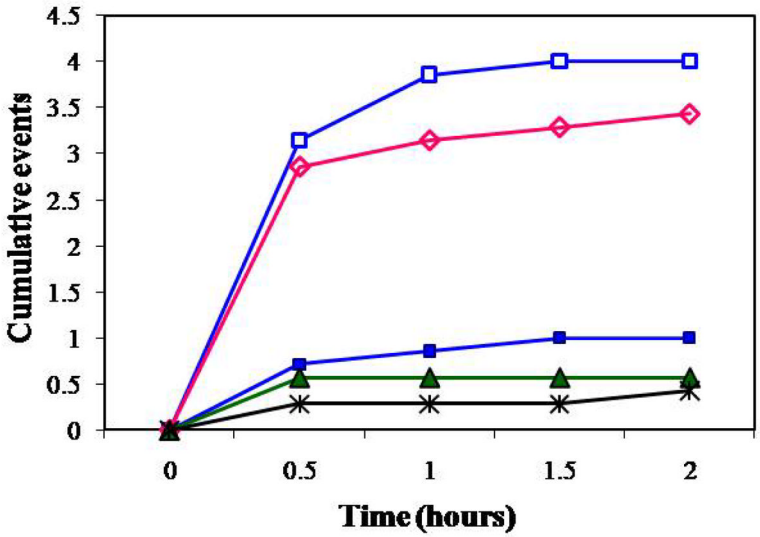

Figure 7.

Transport of nanoparticles synthesized from different polymers in Caco-2-lymphocyte co-cultures. (Closed square = chitosan-DNA nanoparticles, Open square = chitosan-DNA nanoparticles conjugated with transferrin, Open diamond = Gelatin-DNA nanoparticles conjugated with transferrin, Closed triangle = Polystyrene nanoparticles, Cross = PEI-DNA nanoparticles)

Table 1

Physical characteristics of nanoparticles synthesized from various polymers.

Polymer	Size	Zeta potential
HMW chitosan DNA nanoparticles (N/P = 3)	229±63 nm	20±1.2 mV
HMW chitosan DNA nanoparticles with transferrin (N/P = 3)	327±51 nm	35 ±0.8 mV
Gelatin nanoparticles with transferrin	412±120 nm	−10.7±3.9mV
Carboxylated polystyrene beads	200 nm	−51±4.7 mV
Polyethyleneimine (PEI) nanoparticles	121.4 ±7.6 nm	25.7 ±3.5